High Force Unimanual Handgrip Contractions Increase Ipsilateral Sensorimotor Activation and Functional Connectivity

Andrushko, Justin W.; Gould, Layla A.; Renshaw, Doug W.; Ekstrand, Chelsea; Hortobagyi, Tibor; Borowsky, Ron; Farthing, Jonathan P.

Published in:
Neuroscience

DOI:
10.1016/j.neuroscience.2020.10.031

Publication date:
2021

NEUROSCIENCE
RESEARCH ARTICLE

INTERNATIONAL BRAIN IBRO RESEARCH ORGANIZATION

J. W. Andrushko et al. / Neuroscience 452 (2021) 111–125

High Force Unimanual Handgrip Contractions Increase Ipsilateral Sensorimotor Activation and Functional Connectivity

Justin W. Andrushko,[a] Layla A. Gould,[b] Doug W. Renshaw,[a] Chelsea Ekstrand,[c] Tibor Hortobágyi,[d] Ron Borowsky[b,e] and Jonathan P. Farthing[a]*

[a] *College of Kinesiology, University of Saskatchewan, Saskatchewan, Canada*

[b] *College of Medicine, Division of Neurosurgery, University of Saskatchewan, Saskatchewan, Canada*

[c] *The Brain and Mind Institute, Western University, London, Ontario, Canada*

[d] *Center for Human Movement Sciences, University Medical Center Groningen, University of Groningen, Groningen, the Netherlands*

[e] *College of Arts and Science, Department of Psychology, Saskatchewan, Canada*

Abstract—Imaging and brain stimulation studies seem to correct the classical understanding of how brain networks, rather than contralateral focal areas, control the generation of unimanual voluntary force. However, the scaling and hemispheric-specificity of network activation remain less understood. Using fMRI, we examined the effects of parametrically increasing right-handgrip force on activation and functional connectivity among the sensorimotor network bilaterally with 25%, 50%, and 75% maximal voluntary contractions (MVC). High force (75% MVC) unimanual handgrip contractions resulted in greater ipsilateral motor activation and functional connectivity with the contralateral hemisphere compared to a low force 25% MVC condition. The ipsilateral motor cortex activation and network strength correlated with relative handgrip force (% MVC). Increases in unimanual handgrip force resulted in greater ipsilateral sensorimotor activation and greater functional connectivity between hemispheres within the sensorimotor network.

Key words: unimanual handgrip, fMRI, ipsilateral activation, sensorimotor network, functional connectivity.

INTRODUCTION

Imaging and brain stimulation studies provide evidence that our classical understanding of primarily lateralized contralateral motor control offers an incomplete view of unimanual voluntary force generation by identifying widespread sensorimotor brain network activity. Indeed, when healthy humans generate unimanual force, the primary motor cortex (M1) becomes activated in each hemisphere (Hortobágyi et al., 2003; Kobayashi et al., 2003; Zijdewind et al., 2006; Sun et al., 2007; Perez and Cohen, 2008; Hendy et al., 2017). However, the scaling and hemispheric-specificity of network activation with unimanual voluntary force generation remain unclear (Kim et al., 1993; Thickbroom et al., 1998; Kobayashi et al., 2003; Perez and Cohen, 2008; Buetefisch et al., 2014). The key centers that control each upper extremity reside primarily in the opposite cerebral hemisphere (Cincotta and Ziemann, 2008). The contralateral hemisphere projects approximately 90% of descending corticospinal pyramidal tracts across the body through the decussation in the medulla forming the lateral corticospinal tract, with the remaining ~10% of the tracts descending ipsilaterally forming the anterior corticospinal tract (Amaral, 2000). Previous literature proposed that ipsilateral activation could afford additional neural drive for the generation of unimanual force (Kobayashi et al., 2003; Jankowska and Edgley, 2006). However, scientific inquiry into the functional role has been inconsistent, with findings that suggest the ipsilateral M1 (iM1) plays an inhibitory (Kobayashi et al., 2003) and facilitatory (Perez and Cohen, 2008) role in unimanual motor behavior.

Most prior studies that examined ipsilateral brain activity with unilateral motor tasks have used single and paired-pulse TMS measures (Hess et al., 1986; Stedman et al., 1998; Tinazzi and Zanette, 1998; Muellbacher et al., 2000; Hortobágyi et al., 2003; Perez and Cohen, 2008; Vercauteren et al., 2008; Hendy et al., 2017). A potential limitation to utilizing non-invasive brain stimulation to measure the neuromuscular responses is that even with low stimulation intensities, the spatial extent (Doty and Negrão, 1973) and repetitive discharge frequencies (Maier et al., 2013; Lemon and Kraskov, 2019) of the stimulated cortical tissue are much greater than would be under natural conditions (see review by Carson (2020)). Previously, studies have

*Corresponding author. Address: College of Kinesiology, 87 Campus Drive, University of Saskatchewan, Saskatoon, Saskatchewan S7N 5B2, Canada.
E-mail address: jon.farthing@usask.ca (J. P. Farthing).

https://doi.org/10.1016/j.neuroscience.2020.10.031
0306-4522/

utilized fMRI to examine lateralization of brain 'activation' with increased unimanual force generation (Dettmers et al., 1995; Thickbroom et al., 1998; Dai et al., 2001; Van Duinen et al., 2008). With fMRI, brain 'activation' can be determined by examining the blood-oxygen level dependent (BOLD) signal, providing an indication of oxygen uptake by active neurons, which is highly correlated with brain activation (Golkowski et al., 2017). Brain imaging can increase our understanding of the magnitude, hemispheric specificity, and the relationship between activation intensity and temporal correlates (i.e., functional connectivity) of motor centers involved in unimanual voluntary force generation. This is achieved by determining the BOLD signal 'activation' and connectivity between motor centers within and between hemispheres during unimanual motor tasks (Fling et al., 2012; Rosen et al., 2013; Stagg et al., 2014). Hebbian theory suggests neurons that fire together, wire together (Hebb, 1949; Shatz, 1992; Zenke et al., 2017), which is to suggest that if regions of the brain are temporally correlated or '*functionally connected*' they are likely to be functionally involved in the desired behavior (Bi and Poo, 2001). To link the TMS evidence with that of fMRI and MR spectroscopy, there is some evidence to suggest that interhemispheric inhibition (IHI) and functional connectivity are negatively correlated (Fling et al., 2012; Rosen et al., 2013) with higher levels of functional connectivity associated with lower levels of IHI. There is also evidence that a decrease in γ-aminobutyric acid (GABA; inhibitory neurotransmitter) concentration within the contralateral M1 (cM1) correlates with greater functional connectivity across the sensorimotor network bilaterally (Stagg et al., 2014), suggesting that interhemispheric temporal connectivity is enhanced when inhibition is decreased. Therefore, using fMRI to measure functional connectivity and the BOLD signal has the potential to offer insights into interhemispheric and intracortical balance in a non-perturbed state. To our knowledge, no previous fMRI studies have investigated the functional connectivity of the sensorimotor network during forceful unimanual contractions.

The purpose of this study was to determine the effects of parametrically increasing right-handgrip force on activation and connectivity of the sensorimotor network within and between hemispheres. The hypotheses were that (I) BOLD signal in contralateral and ipsilateral sensorimotor areas would increase with greater handgrip forces, and (II) functional connectivity of the sensorimotor network would increase bilaterally during the higher force handgrip contractions, suggesting that neural activity in ipsilateral sensorimotor regions scales with force.

EXPERIMENTAL PROCEDURES

Ethical approval

This study conformed to the standards set by the Declaration of Helsinki and was approved by the University of Saskatchewan Biomedical Research Ethics Boards: Bio# 01-125. Researchers were not blinded during data collection or analyses.

Primary experiment

Participants. Thirteen healthy adults (Data are presented as mean ± standard deviation; 11 right-handed, 2 left-handed, age: 28 ± 6 yrs, height: 170.9 ± 9.8 cm, mass: 75.1 ± 16.7 kg) participated in the study. All participants were screened using an MRI patient safety questionnaire, and handedness was self-reported. Participants were instructed to refrain from exercise for 24 h prior to the MRI session. Written informed consent was obtained from each participant prior to study commencement, and participants were blinded from the study's hypotheses.

Experimental design and fMRI parameters. Participants attended two fMRI sessions where they completed three experimental conditions during each session, involving submaximal unimanual isometric handgrip contractions (25%, 50%, 75% of maximal voluntary contraction [MVC]) with the right hand. Data from two sessions were averaged to reduce variance for each participant in analyses. An MRI-compatible hand clench dynamometer (Biopac Systems Inc. Aero Camino Goleta, CA) was used for this study. All scans were done in a Siemens 3T MAGNETOM Skyra MRI scanner (Siemens Healthcare, Erlangen, Germany). Scanning sessions were separated by a minimum of 48 h. Each session began with whole-brain anatomical scans acquired using a high-resolution magnetization prepared rapid acquisition gradient echo (MPRAGE) sequence consisting of 192 T1-weighted echo-planar imaging slices (1 mm slice thickness with no gap), with an in-plane resolution of 1 × 1 mm (field of view = 256 × 256; repetition time [TR] = 1900 ms; echo time [TE] = 2.08 ms). Following the whole brain anatomical scans, participants performed three right-handed MVCs with 60 s of rest between trials. No brain scans were taken during each MVC. After the maximum handgrip force was determined, the three submaximal handgrip conditions (25%, 50%, 75%) were completed in random order during fMRI brain scans. For each of the functional tasks, T2*-weighted single-shot gradient-echo EPI scans were acquired using an interleaved ascending sequence, consisting of 105 volumes (TR = 1650 ms; TE = 30 ms) of 25 axial slices of 4-mm thickness (1-mm gap) with an in-plane resolution of 2.7 mm × 2.7 mm (field of view = 250) using a flip angle of 90°. The top 2 coil sets (16 channels) of a 20-channel Siemens head-coil (Siemens Healthcare) were used. Scans consisted of a 10-volume alternating block design beginning with five volumes for stabilization (task, rest; 105 volumes total). During scans the participants wore MRI compatible goggles and viewed a projection of a computer screen running a custom-built LabView (version 8.6) interface. Participants saw clear target lines and go/no-go flashing lights and were cued when to contract or relax. The LabView interface was triggered by the MRI to ensure the task was synchronized with each TR.

Behavioral motor task. Participants performed 5 sets × 5 repetitions of grip contractions at each prescribed contraction force during separate scanning runs. In a block design, task blocks composed of 1650 ms (i.e., corresponding to the TR for the T2* imaging) contractions alternating with 1650 ms of rest (16.5 s total task block), separated by rest blocks of complete rest (16.5 s total rest block). Target lines were presented relative to the individual's peak MVC and force feedback was presented as a vertical force bar that was responsive to each participant's grip contraction (i.e., harder contraction resulted in the bar rising vertically). Two virtual 'lights' were present on the motor task interface to cue participants. A green/black light turned green to instruct the participant to contract to the target line and turned black to indicate when to stop contracting. A second red/black light remained black during task blocks and turned red during rest blocks to indicate a sustained rest. The red light switched to black moments before the next task block as an indicator that the next task series of contractions was about to begin. During each contraction force condition, participants were instructed to relax their non-active left arm and hand to prevent mirror activity. Previous research has demonstrated by consciously attempting to relax the non-active limb mirror activity can be negligible or abolished (Hortobágyi et al., 2011).

fMRI pre-processing. Functional MRI data processing was carried out using FMRI Expert Analysis Tool (FEAT) Version 6.00, as part of FSL (FMRIB's Software Library, www.fmrib.ox.ac.uk/fsl) (Jenkinson et al., 2012). For each participant, the T1 structural images from each session were merged into a single mean T1 template. The session two T1 image was first aligned with the T1 image from session one using FMRIB's Linear Image Registration Tool (FLIRT: (Jenkinson and Smith, 2001; Jenkinson et al., 2002)). Next, 'fslmaths' was used to create a mean participant specific T1 structural template. The mean T1 template image was used for registering session one and two functional data in order to avoid asymmetry-induced bias between sessions (Reuter and Fischl, 2011; Reuter et al., 2012). Boundary based registration was used to register the functional image to the high-resolution mean T1 structural template image, followed by registration to standard space images. Registration of the functional images to mean T1 structural template images was carried out using FLIRT: (Jenkinson and Smith, 2001; Jenkinson et al., 2002), and the registration to the standard space images was carried out using FMRIB's Nonlinear Image Registration Tool (FNIRT; (Andersson et al., 2007a, 2007b)).

The following pre-statistic processing was applied: motion correction using Motion Correction FMRIB's Linear Image Registration Tool (MCFLIRT; (Jenkinson et al., 2002)); non-brain removal using Brain Extraction Tool (BET; (Smith, 2002)); spatial smoothing using a Gaussian kernel of FWHM 6 mm; grand-mean intensity normalization of the entire 4D dataset by a single multiplicative factor (Pruim et al., 2015).

Next, Independent Component Analysis Automatic Removal of Motion Artifacts (ICA-AROMA) was used to identify and remove motion-related noise from the functional data (Pruim et al., 2015). Following the ICA-AROMA data clean up, data were high pass temporal filtered with a 0.01 Hz cut off frequency. Time-series statistical analyses were carried out using FMRIB's Improved Linear Model (FILM) with local autocorrelation correction (Woolrich et al., 2001). Z (Gaussianised T/F) statistic images were constructed non-parametrically using Gaussian Random Field theory-based maximum height thresholding with a corrected significance threshold of $p = 0.05$ (Worsley, 2001).

Statistical analysis

Handgrip force. For each of the five task blocks (five contractions in each task block) the mean force was calculated. Next, a mean of the two sessions was determined for each task block and was normalized to the mean MVC force (Mean of session one and two) and expressed as a relative value (% MVC). A condition (25, 50, 75% MVC) × time (blocks 1–5) repeated measures analysis of variance (RM-ANOVA) was used to determine motor performance.

Task-based functional activation. To assess the activation of brain activity in the three conditions, a multi-session and multi-subject repeated measures analysis was carried out. This analysis method involved three levels. First-level analysis involved analyzing individual scans using a binary block design (1's for when activation should occur and 0's for when the participant should be at rest) in the general linear model (GLM). Second-level analysis involved creating across session subject means for each condition using a Fixed Effects voxelwise analysis with a corrected *p*-value threshold of ≤ 0.05. The third level analysis involved analyzing group-level statistics using FMRIB's Local Analysis of Mixed Effects (FLAME) 1 with voxelwise statistical thresholding (corrected *p*-value threshold $\leq$ 0.05). For the third level analysis a '*triple-t*' test was run, which generated three contrast maps (75 > 50% MVC; 75 > 25% MVC; 50 > 25% MVC) to investigate the significant differences between conditions.

Motor cortex region of interest signal change. Regions of interests (ROI) for the M1 in each hemisphere were based on the Brainnetome atlas (cM1: A4ul_l; iM1: A4ul_r) (Fan et al., 2016). A condition (25%, 50%, 75% MVC) × hemisphere (cM1, iM1) RM-ANOVA was used to test for an interaction between conditions and hemisphere for percent signal change. To assess significant main effects and/or the higher order interaction, Bonferroni post-hoc testing was used. Additional data analyses involve separate Spearman's correlations with relative handgrip force (% MVC) and the percent signal change in the cM1 and iM1. Relative handgrip force was entered as a continuous variable using all data from each condition (each participant contributed three data points to the correlation model).

Statistical analyses were carried out in Jamovi version 1.2.16 (The Jamovi Project, 2020) using R version 3.6 (R Core Team, 2019) with packages afex (Singmann, 2018) and emmeans (Lenth, 2018).

Functional connectivity. To assess the functional connectivity of the motor network during the three different contraction force conditions, the 50 volumes corresponding with the task blocks were extracted and merged across time. Rest volumes were removed to avoid the potential impact that rest-related activity may have on the functional connectivity analysis (Steel et al., 2016; Cole et al., 2018). First, a non-constrained dimensionality independent component analysis was carried out using temporal concatenation implemented in Multivariate Exploratory Linear Decomposition into Independent Components (MELODIC) Version 3.15, part of FSL. The non-constrained analysis resulted in 28 independent components. After evaluating the components for fit, it was determined that the 28 components over split the data and reducing the number to 10 components prevented over splitting of known spatial networks. Spatial networks were cross-correlated with known spatial distributions (Smith et al., 2009) to confirm that constraining the ICA to 10 components appropriately identified known networks.

Data were masked to remove non-brain voxels; voxel-wise de-meaned; normalized for the voxel-wise variance; whitened (remove the temporal autocorrelation resulting from intrinsic smoothness in voxel time-series data) and projected into a dimensional subspace using probabilistic Principal Component Analysis. Laplace approximation was used to estimate the number of dimensions in the data (Minka, 2000; Beckmann and Smith, 2004). The whitened observations were temporally decomposed into sets of time-series vectors; the participant domain, and across the spatial domain (maps). This was achieved by optimizing for non-Gaussian spatial source distributions using a fixed-point iteration technique (Hyvärinen, 1999). Estimated component maps were divided by the standard deviation of the residual noise, and a threshold was determined by fitting a mixture model to the histogram of intensity values (Beckmann and Smith, 2004).

All three conditions across both sessions (78 total scans) were included in the group level map at the MELODIC stage. Between condition contrasts were carried out using dual regression with exchangeability blocks used to pair within-subject runs for the permutation testing to determine the null distribution (i.e., three conditions across both sessions were included in one exchangeability block for each participant) (Nickerson et al., 2017). Dual regression involves three stages. First, the concatenated fMRI dataset from the MELODIC stage was decomposed into the 10 predefined spatial maps (determined from the group level ICA analysis) resulting in a 4D space–time dataset with 10 independent timeseries for each participant. Second, the 10 independent time-series were regressed as temporal regressors in a multiple regression, into the same 4D dataset resulting in 10 spatial maps for each participant (one spatial map for each group-level component). The network of interest was then split into individual runs using '*fslsplit*', then for each condition the runs were averaged across sessions for each individual using '*fslmaths*'. For each participant and condition, the mean of the two sessions for the network of interest were then merged back together using '*fslmerge*' resulting in 39 imaging files (13 participants with three conditions each) rather than the original 78 files (13 participants, three conditions with two sessions). Finally, an across condition *F*-test, condition means, and differences between conditions (75 > 50% MVC; 75 > 25% MVC; 50 > 25% MVC) were tested using permutation-testing with FSL's tool *randomise* using threshold-free cluster enhancement (TFCE) statistics (Smith and Nichols, 2009). The sensorimotor network and the default mode network were assessed with this approach. The default mode network was assessed as a control measure to ensure data stability between the three conditions in a non-task related network. A manual Bonferroni correction was used to adjust the alpha level for statistical significance in order to correct for the comparison of multiple components ($\alpha = 0.025$; [0.05/2]).

An ROI approach was used to determine the network strength (i.e., parameter estimates) of the cM1 and iM1 for each individual and condition. The same Brainnetome atlas ROI masks used on the functional activation data were used for the functional connectivity analyses (cM1: A4ul_l; iM1: A4ul_r) (Fan et al., 2016). The network strength provides an indication of each individual's 'contribution' to the overall group level sensorimotor network, whereby a larger parameter estimate indicates that a given individual or condition has stronger functional connectivity to the rest of the network. A condition (25%, 50%, 75% MVC) $\times$ hemisphere (cM1, iM1) RM-ANOVA was used to test for interactions between conditions and hemisphere for network strength. Bonferroni post-hoc tests were used to assess significant main effects and/or the higher order interaction. Further data analyses involved using separate Spearman's correlations to determine if relative handgrip force correlated with the overall network strength, and cM1 and iM1 network strength.

Control experiment

Participants. A separate cohort of 11 right-handed participants (age: 30.6 ± 6.1 yrs, height: 176.3 ± 31.7 cm, mass: 81.2 ± 34.2 kg) were recruited to participate in a single session control experiment where the same submaximal tasks (25%, 50% and 75% MVC) were performed with EMG recordings of the wrist flexor muscles in each arm. The setup was similar to the MRI environment, with participants laying supine while watching a computer screen during task performance. Participants were instructed to limit body movement during the tasks. The purpose of the control experiment was to quantify muscle activity in the active and non-active arms during the handgrip task.

Muscle activity acquisition. EMG electrodes (VERMED NeuroPlus; 2.5 cm^2, Ag/Ag) were placed over the flexor carpi radialis (FCR) muscles in each arm. Electrodes were placed one-third of the distance from the medial epicondyle to the radial styloid following the recommendations from Buschbacher and Prahlow (2000) and Zehr (2002). EMG data was recorded using Biopac amplifier MP150 (Biopac Systems Inc. Aero Camino Goleta, CA) with a sampling rate of 2000 Hz.

EMG processing. The EMG signal from each MVC and the submaximal conditions were demeaned, then filtered with a fourth order Butterworth digital filter with a high-pass cut-off of 10 Hz, and a low-pass cut-off of 500 Hz. The root–mean–square (RMS) of the filtered EMG signal was then calculated with a moving RMS (window length of 250 ms). The onset and offset of each of the 25 contractions over the course of the five task blocks were determined. The mean RMS EMG for each contraction was then normalized to the mean RMS of the EMG from the peak MVC for each arm respectively (left arm EMG normalized to left arm MVC, right arm EMG normalized to right arm MVC). There were two missing data points across all participants, due to two separate participants missing a repetition when visually cued, this resulted in 24 total contractions for a given condition. The missing data points were replaced with the median value for the given repetition within the respective condition. Next, a within subject normality assessment was conducted using a Kolmogorov–Smirnov test. Where violated, outlier data points were assessed, removed and replaced with median values. After outlier removal, for each participant the mean normalized EMG activity for each block (five contractions) was calculated for each condition. The mean values were then carried forward for analysis using a condition (25%, 50%, 75% MVC) × time (five blocks) RM-ANOVA. Where there were violations to sphericity, a Greenhouse-Geisser correction was used.

RESULTS

Primary experiment

Behavioral task. Mean handgrip MVC force across the two sessions was 43.6 ± 15.6 kg-Force. Participants were accurate with the motor task performance at 25% MVC (Relative: 26.1 ± 1.9% MVC; Absolute: 11.4 ± 4.3 kg-Force) and 50% MVC (Relative: 51.3 ± 4.1% MVC; Absolute: 22.3 ± 7.8 kg-Force). However, the 75% MVC condition was a mean 5% under their target value (Relative: 69.9 ± 8.3% MVC; Absolute: 30.7 ± 12.0 kg-Force).

A significant condition × time interaction was observed, Greenhouse-Geisser corrected $F(1.646, 19.746) = 4.819$, $p = 0.025$, $\eta_p^2 = 0.287$, in addition to main effects of condition (Greenhouse-Geisser corrected, $F(1.042,12.509) = 168.454$, $p < 0.001$, $\eta_p^2 = 0.934$), and time (Greenhouse-Geisser corrected, $F(1.461,17.527) = 2.773$, $p = 0.102$, $\eta_p^2 = 0.188$).

Task-based functional activation. Contrasts. Three contrasts were analyzed (75% > 50% MVC; 75% > 25% MVC; 50% > 25% MVC). Contrast maps between 75 > 50% MVC and 50 > 25% MVC failed to detect significant differences between conditions. The 75 > 25% MVC contrast map revealed several significant clusters of activation (Fig. 1; Table 1). Regarding the motor related areas of the cerebrum, a notable cluster of activation was observed over the iM1 hand knob region. Suggesting that the 75% MVC condition resulted in a stronger BOLD signal in the iM1 compared to the 25% MVC condition (Table 1). For non-threshold magnitude difference images (contrast of

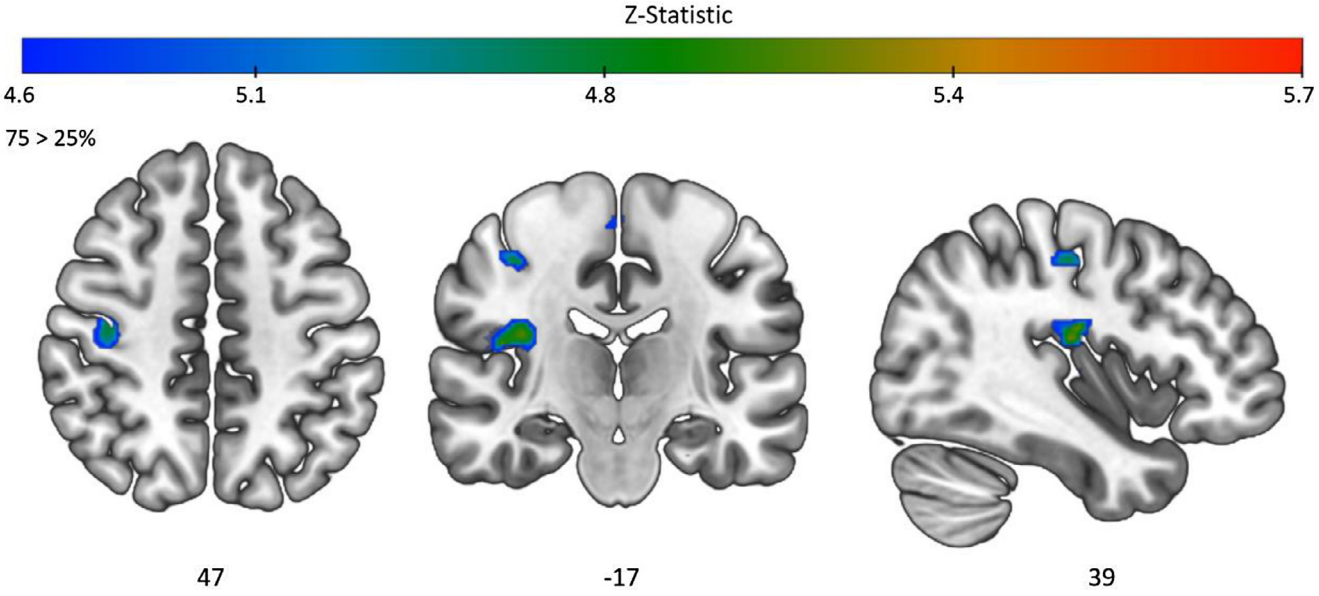

Fig. 1. 75 > 25% MVC contrast map for the 105-volume block design activation analysis. Threshold $z = 4.6$ ($p < 0.05$). Figure is in radiological view (left side of brain on the right; right side of brain on the left).

Table 1. Condition activation contrast maps. Peak *Z*-statistic voxel for significant clusters

75 > 50% MVC					
Voxels	*Z*-MAX	*Z*-MAX MNI Coordinates (mm)			AAL Label
		X	*Y*	*Z*	
2	5.02	−2	68	2	Frontal Superior Medial Left
1	4.82	8	−42	20	Cingulum Post Right
75 > 25% MVC					
Voxels	*Z*-MAX	*Z*-MAX MNI Coordinates (mm)			AAL Label
		X	*Y*	*Z*	
293	5.61	10	−88	34	Cuneus Right
267	5.55	36	−16	18	Insula Right
112	5.29	38	−16	48	Precentral Right
67	5.13	0	−20	64	Supplementary Motor Area Right
47	5.35	62	4	2	Temporal Pole Superior Right
36	5.21	8	−34	−40	Cerebellum 9 Right
32	5.87	18	−4	−2	Pallidum Right
25	4.78	−6	−92	8	Calcarine Left
20	5	36	−22	68	Precentral Right
19	4.81	−56	−6	28	Postcentral Left
17	5.23	−20	2	−14	Amygdala Left
16	4.89	−12	−40	−20	Cerebellum 4 5 Left
10	4.82	−40	−6	−18	Fusiform Left
7	5.04	−70	−36	−4	Temporal Middle Left
5	5.1	−10	60	−6	Frontal Medial Orbital Left
5	4.75	6	−24	−24	Cerebellum 3 Right
4	4.69	4	−92	16	Cuneus Left
3	4.94	−42	−8	−12	Temporal Superior Left
3	4.68	8	−20	48	Cingulum Middle Right
3	4.86	42	54	30	Frontal Middle Right
3	4.84	54	46	10	Frontal Inferior Triangular Right
2	4.66	52	−12	56	Precentral Right
2	4.8	−26	−18	−26	ParaHippocampal Left
2	4.86	−2	68	22	Frontal Superior Medial Left
2	4.72	−54	−12	20	Postcentral Left
2	4.75	−50	−16	16	Rolandic Operculum Left
2	4.78	40	−14	6	Insula Right
2	4.81	10	−26	−16	Cerebellum 3 Right
2	5.03	−2	68	2	Frontal Superior Medial Left
2	4.72	4	−20	−8	Thalamus Right
2	4.73	−28	−24	−6	Hippocampus Left
2	4.66	−10	−28	72	Paracentral Lobule Left
1	4.71	62	6	12	Rolandic Operculum Right
1	4.69	−10	64	36	Frontal Superior Left
1	4.68	2	−82	−6	Calcarine Left
50 > 25% MVC					
Voxels	*Z*-MAX	*Z*-MAX MNI Coordinates (mm)			AAL Label
		X	*Y*	*Z*	
None.					

parameter estimates) between the three conditions see Fig. 2 (Chen et al., 2017).

Region of interest analysis – activation. For the percent BOLD signal change within each ROI, a significant main effect of hemisphere, $F(2,24) = 139.73$, $p < 0.001$, $\eta_p^2 = 0.921$ and a condition × hemisphere interaction was observed, $F(2,24) = 6.60$, $p = 0.005$, $\eta_p^2 = 0.355$. The main effect of condition was not significant, $F(2,24) = 3.18$, $p = 0.059$, $\eta_p^2 = 0.209$. BOLD signal change was significantly larger in the cM1 compared to the iM1, with a mean signal change difference of 0.52%. To understand the interaction, data for each hemisphere were split, and conditions

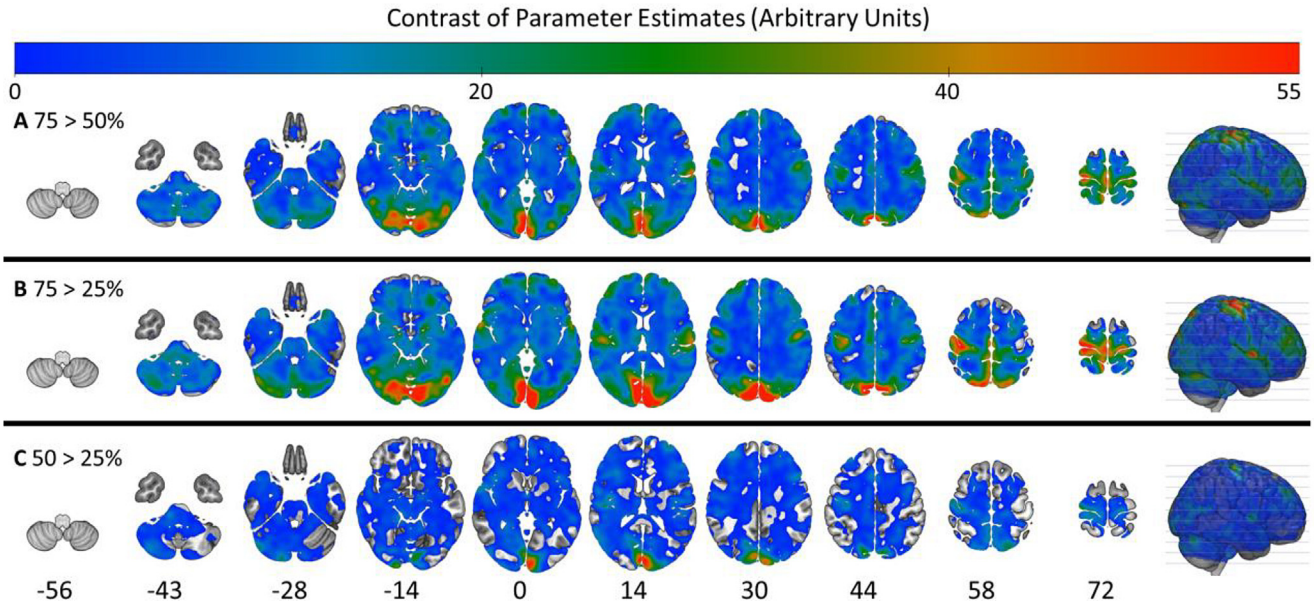

Fig. 2. Non-threshold brain activation magnitude difference maps. Color bar represents the contrast of the parameter estimates for **(A)** 75 > 50% MVC, **(B)** 75 > 25% MVC, and **(C)** 50 > 25% MVC conditions. Figure is in radiological view (left side of brain on the right; right side of brain on the left).

compared. A RM-ANOVA for the cM1, failed to observe a significant condition main effect, $F(2,24) = 0.682$, $p = 0.515$, $\eta_p^2 = 0.054$ indicating that the percent signal chance in the cM1 was not different between conditions. However, a RM-ANOVA for the iM1 revealed a significant main effect of condition, $F(2,24) = 9.393$, $p < 0.001$, $\eta_p^2 = 0.439$. Bonferroni post-hoc tests demonstrated that iM1 signal change in the 75% condition was greater than 25% ($p < 0.001$) and 50% ($p = 0.017$), but 50% and 25% conditions were not significantly different ($p = 0.784$).

iM1 signal change (Brainnetome atlas; A4ul_r). Relative handgrip force (% MVC) was significantly correlated with the iM1 signal change, $\rho(38) = 0.553$, $p = 0.001$, 95% confidence interval (CI): 0.279–0.744 (Fig. 3A).

cM1 signal change (Brainnetome atlas: A4ul_l). Relative handgrip force (% MVC) was not correlated with cM1 signal change, $\rho(38) = 0.210$, $p = 0.199$, 95% CI: −0.122 to 0.500 (Fig. 3B)

On-task functional connectivity. Sensorimotor network contrasts. The 1 minus family wise error rate (1-FWE) corrected *p*-value statistical maps generated from *randomise* with TFCE statistical processing reveal a significant difference in the left, contralateral hemisphere over the pre- and postcentral gyrus (Table 2). This significant cluster of stronger network connectivity is lost after the Bonferroni correction. A total of six significant clusters were present in the 75% > 25% MVC connectivity contrast within the sensorimotor network. Of interest to the hypothesis, the strongest cluster resides over the ipsilateral precentral gyrus, indicating that higher force handgrip contractions, specifically 75% compared to 25% MVC, increases the sensorimotor network functional connectivity between the ipsilateral

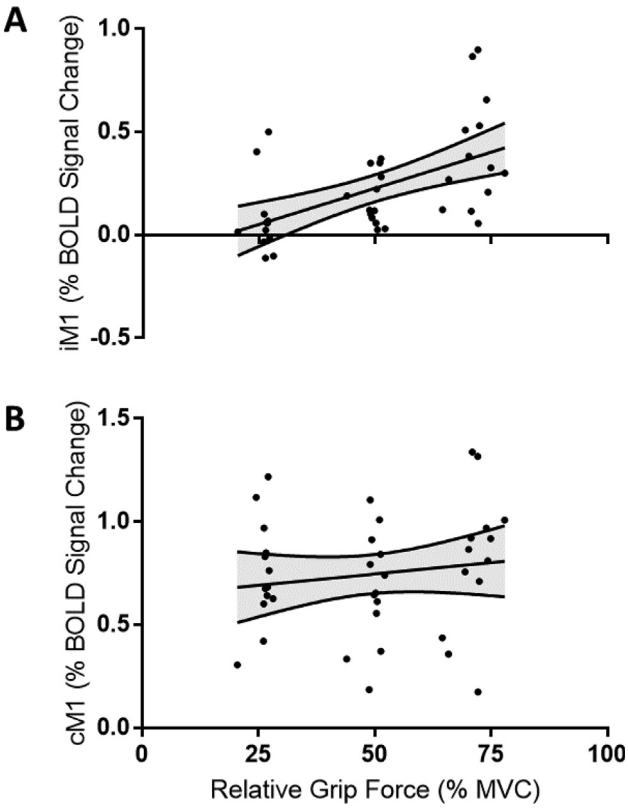

Fig. 3. Region of interest analyses for the percent BOLD signal change of the contralateral (cM1; Brainnetome atlas: A4ul_l) and ipsilateral hand/arm region of the motor cortex (iM1: Brainnetome atlas: A4ul_r). Spearman's correlations were run with relative handgrip force (% MVC) and: **(A)** ipsilateral motor cortex, $\rho(38) = 0.553$, $p = 0.001$, and **(B)** contralateral motor cortex, $\rho(38) = 0.210$, $p = 0.199$. Scatter plots display 95% confidence intervals around the slope (gray band).

Table 2. Sensorimotor network connectivity contrast maps. Peak *P*-statistic voxel for significant clusters

75 > 50% MVC					
Voxels	*P*-MAX	*P*-MAX MNI Coordinates (mm)			AAL Label
		X	*Y*	*Z*	
25	0.034	50	12	34	Postcentral left
75 > 25% MVC					
Voxels	*P*-MAX	*P*-MAX MNI Coordinates (mm)			AAL Label
		X	*Y*	*Z*	
538	0.007*	26	24	74	Precentral Right
75	0.018*	50	12	28	Postcentral Left
18	0.04	14	30	62	Paracentral Lobule Left
4	0.038	20	76	42	Cerebellum Crus 2 Left
2	0.047	22	24	76	Postcentral Left
1	0.05	22	28	78	Postcentral Left
50 > 25% MVC					
Voxels	*P*-MAX	*P*-MAX MNI Coordinates (mm)			AAL Label
		X	*Y*	*Z*	
None					

* Significant at Bonferroni corrected = 0.025.

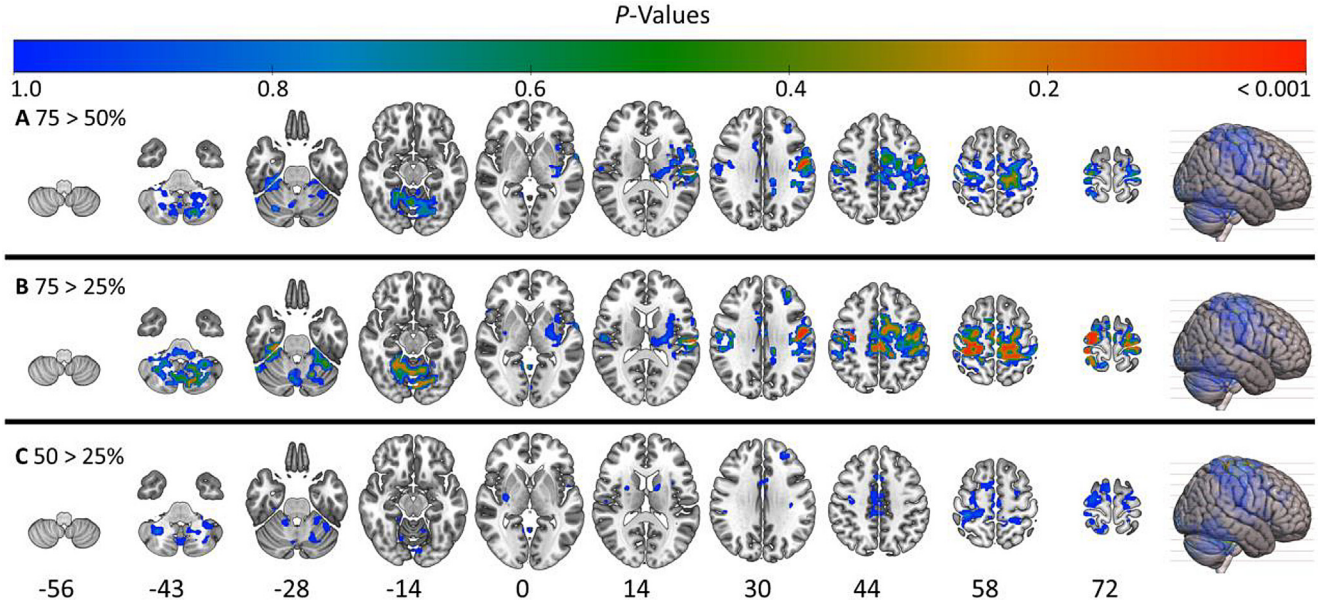

Fig. 4. Sensorimotor network functional connectivity contrast maps for **(A)** 75 > 50% MVC, **(B)** 75 > 25% MVC, and **(C)** 50 > 25% MVC conditions. There were significant differences between **(B)** 75 > 25% MVC conditions after Bonferroni corrections. Figure is in radiological view (left side of brain on the right; right side of brain on the left).

and contralateral hemispheres. There were no significant differences observed between 50% and 25% conditions (Fig. 4).

Region of interest analysis – sensorimotor network connectivity. For network strengths within each ROI, the condition × hemisphere interaction did not reach significance, $F(2,24) = 0.114$, $p = 0.893$, $\eta_p^2 = 0.009$. However, main effects of condition ($F(2,24) = 6.842$, $p = 0.004$, $\eta_p^2 = 0.363$) and hemisphere ($F(2,24) = 79.733$, $p < 0.001$, $\eta_p^2 = 0.869$) were observed. Significant differences were found between 75% and 50% conditions (mean difference = 11.531, $t(24) = 2.635$, $p = 0.037$) and 75% and 25% conditions (mean difference = 15.605, $t(24) = 3.566$, $p = 0.004$), but no difference was observed between 50% and 25% conditions, (mean difference = 4.074, $t(24) = 0.931$, $p = 0.626$). As expected for the main effect of

hemisphere, the cM1 network strength was stronger in magnitude than the iM1 (mean difference = 30.893 arbitrary units).

Sensorimotor network strength. Relative handgrip force (% MVC) was significantly correlated with the sensorimotor network strength, $\rho(38) = 0.393$, $p = 0.013$, 95% CI: 0.079–0.6362 (Fig. 5A).

iM1 network strength (Brainnetome atlas; A4ul_r). Relative handgrip force (% MVC) was significantly correlated with the iM1 network strength, $\rho(38) = 0.528$, $p < 0.001$, 95% CI: 0.246–0.728 (Fig. 5B).

cM1 network strength (Brainnetome atlas: A4ul_l). Relative handgrip force (% MVC) was significantly correlated with the cM1 network strength, $\rho(38) = 0.379$, $p = 0.017$, 95% CI: 0.062–0.626 (Fig. 5C).

Default mode network contrasts. The default mode network was analyzed as a control measure for data stability in a non-motor related network. The contrast analyses from *randomise* with TFCE statistical processing failed to reveal any significant differences between the three conditions for the on-task functional connectivity of the default mode network, indicating stability of the network with parametric increase in handgrip force (Fig. 6).

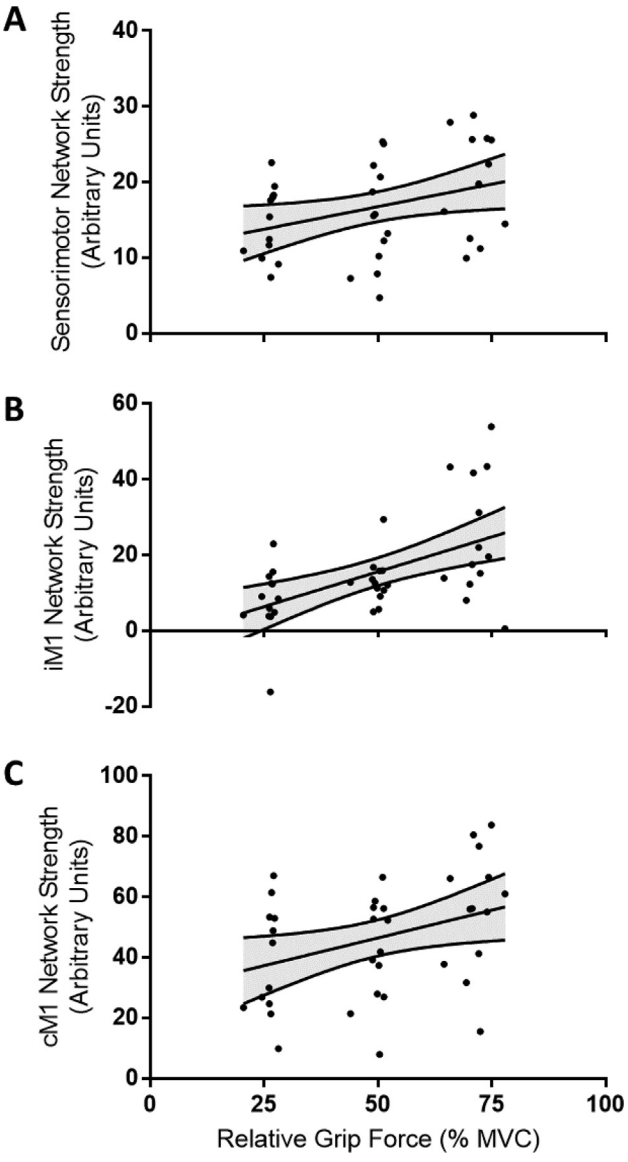

Fig. 5. Region of interest Spearman's correlations for relative handgrip force (% MVC) and the functional connectivity network strengths of **(A)** the entire sensorimotor network, $\rho(38) = 0.393$, p = 0.013, **(B)** ipsilateral motor cortex (iM1; Brainnetome atlas, A4ul_r), $\rho(38) = 0.528$, $p < 0.001$, and **(C)** contralateral motor cortex (cM1: Brainnetome atlas, A4ul_l), $\rho(38) = 0.379$, $p = 0.017$. Scatter plots display 95% confidence intervals around the slope (gray band).

Control experiment

Right active arm force. There was a significant condition × time interaction, $F(8,40) = 3.192$, $p = 0.003$, $\eta_p^2 = 0.242$ and a significant Greenhouse-Geisser corrected condition main effect, $F(1.0,10.1) = 166.534$, $p < 0.001$, $\eta_p^2 = 0.943$. The main effect of time did not reach statistical significance, Greenhouse-Geisser corrected $F(1.827,18.266) = 1.285$, $p = 0.298$, $\eta_p^2 = 0.114$. To break down the significant interaction, post-hoc tests were used to determine that the 75% condition had a significant decrease in handgrip force in the fifth block (block 1 vs. 5, $p = 0.006$). There were no other significant differences over time for any of the conditions. Post-hoc testing for the main effect of condition was used to determine that 25% (Marginal mean = 10.6 ± 2.8 kg-Force), 50% (Marginal mean = 20.3 ± 5.3 kg-Force) and 75% (Marginal mean = 29.3 ± 7.6 kg-Force) MVC conditions were all significantly different from each other (all $p < 0.001$).

Right active arm EMG. There was a significant main effect of condition, Greenhouse-Geisser corrected $F(1.145,11.446) = 30.928$, $p < 0.001$, $\eta_p^2 = 0.756$. However, the condition × time interaction (Greenhouse-Geisser corrected $F(1.497,14.970) = 0.663$, $p = 0.488$, $\eta_p^2 = 0.062$) and main effect of time ($F(1.525,15.249) = 1.455$, $p = 0.259$, $\eta_p^2 = 0.127$) failed to reach significance. Post-hoc testing for the main effect of condition was used to determine that 25% MVC (Marginal mean = 0.291 ± 0.234 MVC) was significantly different than 50% (Marginal mean = 0.535 ± 0.097 MVC, $p = 0.001$), and 75% (Marginal mean = 0.742 ± 0.045 MVC, $p < 0.001$) MVC conditions. Additionally, 50% was also significantly different than the 75% MVC condition ($p = 0.005$) (see Fig. 7A).

Left inactive arm EMG – mirror activity. The condition × time interaction failed to reach significance, Greenhouse-Geisser corrected $F(1.915,19.151) = 0.771$, $p = 0.471$, $\eta_p^2 = 0.072$. Additionally, main effects of condition ($F(2,20) = 1.323$, $p = 0.289$, $\eta_p^2 = 0.117$) and time (Greenhouse-Geisser corrected $F(1.615,16.153) = 2.023$, $p = 0.170$, $\eta_p^2 = 0.168$) also failed to reach significance, indicating that the mean normalized RMS of the EMG signal for the 25% (Marginal mean = 0.025 ± 0.027 MVC), 50% (Marginal mean = 0.020 ± 0.013 MVC) and 75% (Marginal

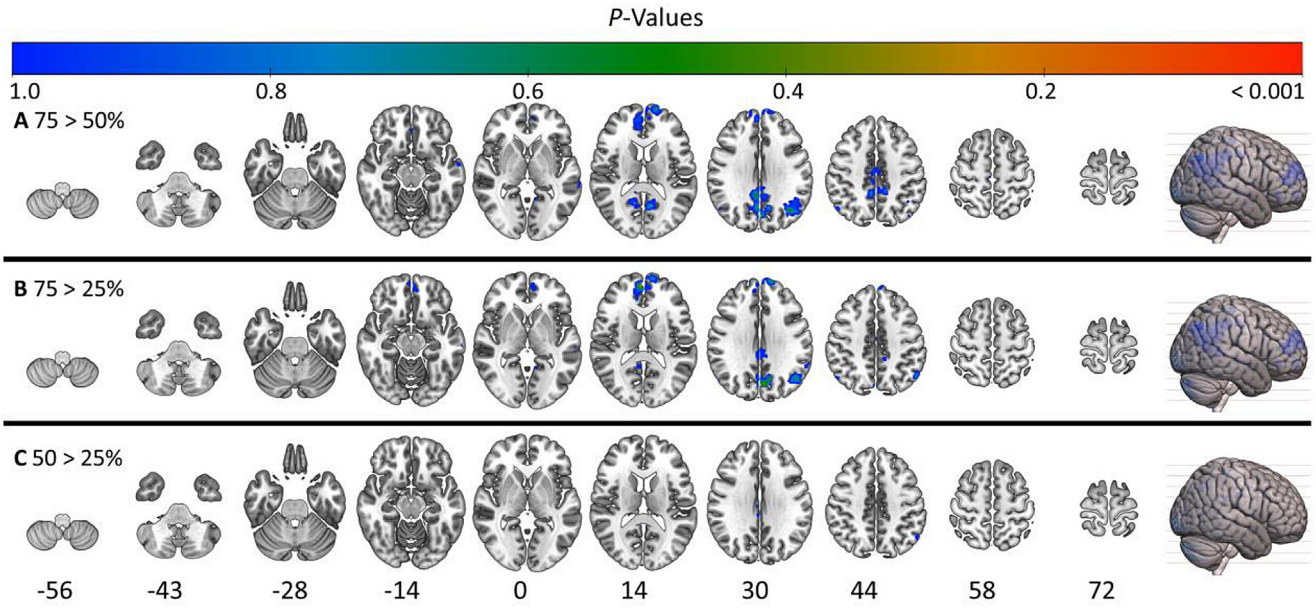

Fig. 6. Default mode network functional connectivity contrast maps for **(A)** 75 > 50% MVC, **(B)** 75 > 25% MVC, and **(C)** 50 > 25% MVC conditions. Figure is in radiological view (left side of brain on the right; right side of brain on the left). There were no significant contrasts.

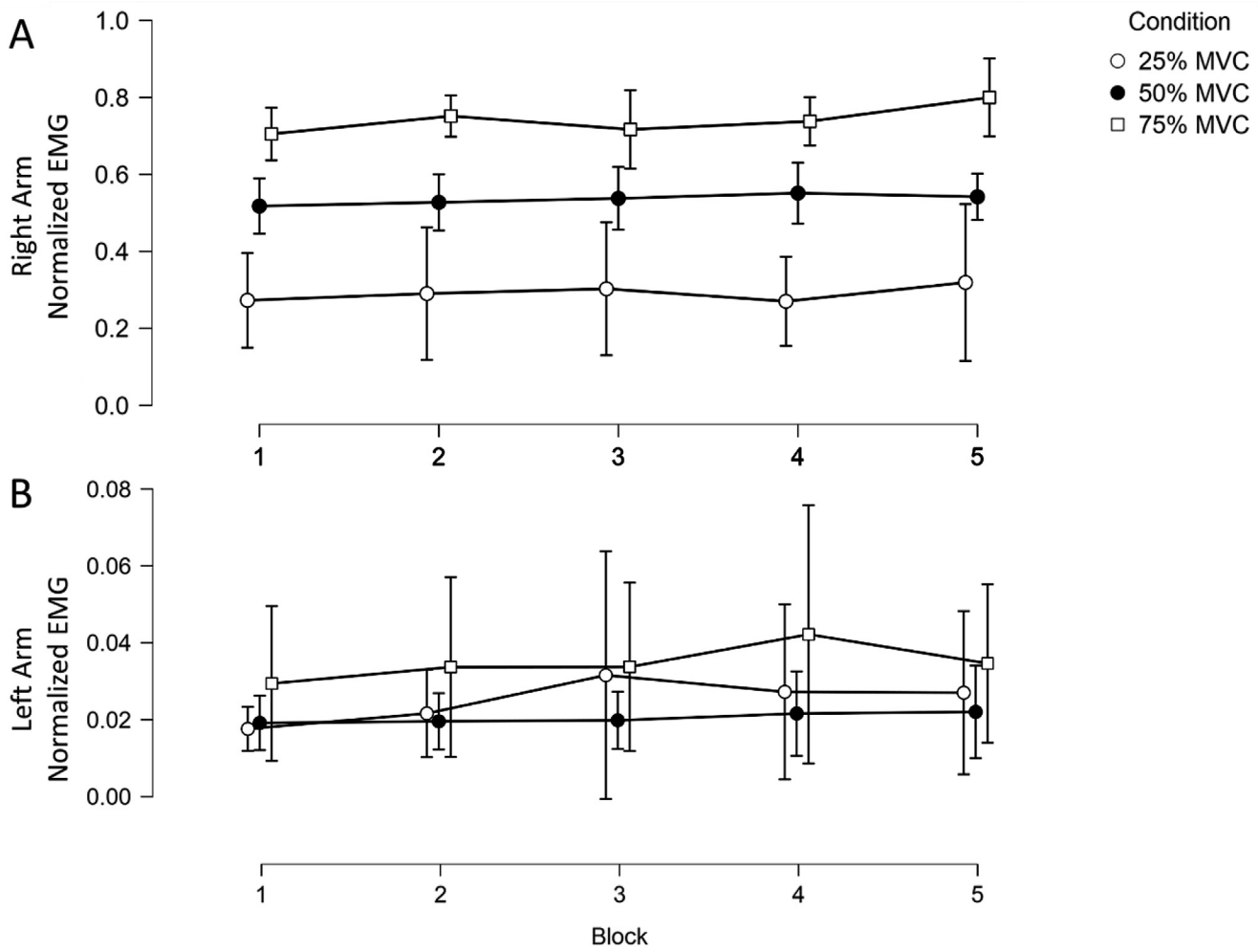

Fig. 7. Control experiment. EMG normalized to MVC for **(A)** the right, active arm, and **(B)** the left, non-active arm for each of the three conditions (25%, 50%, 75% MVC) across the five task blocks. Error bars = 95% confidence intervals.

mean = 0.035 ± 0.035 MVC) were not different (see Fig. 7B).

An additional analysis was carried out with the left arm EMG data without median replacements of missing data points, to ensure the findings are robust and not influenced by the data replacement method. For this analysis the condition × time interaction failed to reach significance, Greenhouse-Geisser corrected $F(1.555,15.548) = 0.525$, $p = 0.557$, $\eta_p^2 = 0.050$. The main effects of condition ($F(2,20) = 1.740$, $p = 0.201$, $\eta_p^2 = 0.148$) and time ($F(1.286,12.859) = 2.050$, $p = 0.176$, $\eta_p^2 = 0.170$) also failed to reach significance.

Left inactive arm baseline EMG. For the baseline EMG signal recorded from the left arm, the mean normalized baseline noise in the EMG signal for the 25% MVC was 0.014 ± 0.005, for 50% MVC was 0.016 ± 0.006, and for the 75% MVC condition was 0.016 ± 0.009.

To assess whether the EMG signal during contractions differed from the baseline noise a 3 × 6 condition (25%, 50%, 75% MVC) × time (Baseline noise, blocks 1–5) RM-ANOVA was run for the left arm normalized EMG signal. There was a significant main effect of time, $F(5,50) = 3.195$, $p = 0.014$, $\eta_p^2 = 0.242$. However the condition × time interaction ($F(10,50) = 0.944$, $p = 0.496$, $\eta_p^2 = 0.086$) and the main effect of condition ($F(2,20) = 1.345$, $p = 0.283$, $\eta_p^2 = 0.119$) failed to reach significance. Bonferroni post-hoc testing for the main effect of time failed to detect any significant differences (All $p > 0.05$). These data suggest that the mirror activity across the three conditions was not significantly different than the baseline noise recorded prior to starting the motor task.

DISCUSSION

To our knowledge, this is the first study to examine the effects of parametrically increasing unimanual handgrip force on activation and 'on-task' functional connectivity (i.e., functional connectivity during task blocks only) within the sensorimotor network and specifically within the primary motor cortices bilaterally (cM1, iM1).

Concurrent bilateral sensorimotor activity, specifically in the iM1 during unimanual motor tasks, has been investigated in several prior studies utilizing TMS or neuroimaging techniques (Hortobágyi et al., 2003; Zijdewind et al., 2006; Perez and Cohen, 2008; Hendy et al., 2017) and has been inconsistently observed in neuroimaging studies. The inconsistent observation is likely due to the differences in the type of task being performed (Buetefisch et al., 2014). There is evidence to suggest that the iM1 activity depends on task complexity (Verstynen et al., 2005; Buetefisch et al., 2014). Verstynen et al. (2005) observed greater iM1 brain activation with complex movements such as sequenced movements with multiple fingers compared to a single finger tapping task. Further, greater iM1 activation was also observed with a more difficult sequence compared to an easier one, suggesting that the complexity of the movement and cognitive demand both recruited iM1 greater than a simpler finger tapping task. The handgrip task employed in the present experiments differed in that the task itself did not change, rather only the requisite force output to achieve the targets changed between conditions. An increase in both ipsilateral and contralateral sensorimotor areas BOLD signal may support the notion that the ipsilateral hemisphere aids the contralateral sensorimotor network to enhance force output under high force conditions (Jiang et al., 2012), but this remains an untested hypothesis, and the purpose of ipsilateral cortical activity remains controversial (Kobayashi et al., 2003). The present study sought to investigate the neural correlates within the sensorimotor network, and more specifically, the activation and network connectivity strength of the cM1 and iM1 with parametrically increasing handgrip contraction forces. The novel data from the current study suggest that both the magnitude of 'activation' and connectivity strength within the iM1 scales with increasing force of unimanual handgrip contractions (Figs. 3 and 5).

For the 75 > 25% MVC activation map there were several clusters of significantly greater activation. Within the cerebral sensorimotor network there were significant clusters covering the iM1 hand knob area, the ipsilateral premotor area and one covering the supplementary motor area bilaterally. Another notable cluster was observable in the occipital lobe. It is possible that the 75% MVC condition preferentially activated the visual cortex in the occipital lobe to a greater extent than the 25% MVC condition. For each condition, the force feedback bar displayed the full range from 0 to 100% MVC, with only the target line changing. With a target line at 75% MVC compared to 25% MVC, the visual force feedback bar that represents the contraction is larger for the higher force condition and provided a greater visual stimulus. Another perhaps more plausible interpretation for the cluster of activation in the occipital lobe is that the cluster is in the vicinity of the superior sagittal sinus and the Torcular Herophili (confluence of sinuses) which is the intersection for the superior sagittal sinus, straight sinus, transverse sinuses and the occipital sinus. False activations are common in this area and around other veins (Salimi-Khorshidi et al., 2014; Eklund et al., 2019), and therefore any interpretation of the activation contrasts in the occipital lobe should be made with caution. Outside of the 75 > 25% contrast, there were two significant clusters in the 75 > 50% MVC contrast, one in the frontal superior medial gyrus and another in the posterior cingulum. Aside from those two small clusters (two and one voxel respectively), no other differences were observed in the 75 > 50% or 50 > 25% MVC activation contrasts.

Importantly, prior work has reported robust iM1 activation with motor tasks requiring substantially less force than the 25% MVC condition in the present study but with greater task complexity (Buetefisch et al., 2014; Uehara and Funase, 2014). In relation to the ipsilateral activation with task complexity, an increase in contraction force, although not necessarily more complex in terms of the motor task itself compared to previous work investigating brain activation with task complexity (Verstynen et al., 2005), resulted in greater ipsilateral activation

(Fig. 1). Anecdotally, participants reported higher task difficulty with the 50% and 75% MVC gripping task, and therefore an increase in task demand may require greater neural activity to suppress unwanted motor behaviors (e.g. reciprocal inhibition) or reflect activation of synergistic muscles (Perez and Cohen, 2008), which could be a driving factor for the ipsilateral activation. Unfortunately, the lack of peripheral measures of muscle activity with EMG in the primary experiment prevents us from directly linking the ipsilateral brain data to resting limb muscle activity, but there is a convincing relationship between the recorded increase in right handgrip force and signal change in the ipsilateral, right, M1 (Fig. 3).

The data from the control experiment suggest that the mirror activity in the left, non-active arm did not scale with the right, active arm. Significant parametric increases in right arm EMG activity were observed, similar to the target force output for each condition (25% condition = 29.103% normalized EMG; 50% condition = 53.527% normalized EMG; 75% condition = 74.239% normalized EMG). Yet there were no significant differences between conditions in the left, non-active arm. Mirror activity was low, ranging from 2 to 3.5% of MVC across the three conditions. Although these data are not definitive, the mirror activity in the control experiment was quantifiably low and therefore we suggest that the ipsilateral brain activation observed in the primary experiment is unlikely to be driving motoneuron activation of the non-active arm.

An additional consideration is the involvement of muscle fatigue in the higher force conditions. Previous literature has demonstrated that in the presence of muscular fatigue, cortical excitability (Aboodarda et al., 2016), functional connectivity (Jiang et al., 2012) and EMG amplitude (Enoka and Duchateau, 2008) increase, whereas intracortical inhibition via TMS (Maruyama et al., 2006; Takahashi et al., 2009) decreases in the iM1. The increase in the 'on-task' functional connectivity observed in the iM1 with greater handgrip force, paired with the small decrease in force output across time for the 75% MVC condition in the control experiment may be an indication that the higher force contractions resulted in some level of muscular fatigue. However, in the control experiment the EMG data did not change over time, within a condition, suggesting muscle fatigue did not alter muscle activation. Investigating the contribution of fatigue within a similar paradigm remains an empirical question for future work.

We show that when healthy humans perform high force handgrip contractions, ipsilateral and contralateral sensorimotor areas activate, coupled with an increase in the functional connectivity within the sensorimotor network. Further, the iM1 activation and network strength scales with grip force in a manner different from the cM1. In the primary experiment there was a notable lack of scaling within the cM1 with parametric increases in handgrip force. It is plausible that in the specific handgrip task, the cM1 contribution was near maximized with the 25% MVC condition, and greater force output within the 50% and 75% conditions was a result of iM1 or other cortical centers contributing to the increased force output. The increase in 'on-task' functional connectivity across the sensorimotor network including cM1 and iM1 (Fig. 5) may lend support for this notion, as an increase in handgrip force resulted in greater synchronicity between sensorimotor areas in each hemisphere, which may have aided in force output. It should be noted however that this is a hypothesis that these data are unable to directly address and warrants further investigation.

LIMITATIONS AND FUTURE DIRECTIONS

Future research may benefit from utilizing MR spectroscopy, electro-encephalography, or magnetoencephalography to gain better insight into the functional premise of ipsilateral brain activity and functional connectivity during unimanual motor behavior. We recorded contraction force and EMG during the movements in a control experiment with a different cohort of participants outside of the MRI. This allowed us gain insight into the potential involvement of mirror activity in the non-active arm. Although, an extension of this work requires the careful examination of EMG muscle activity and the force profile of the homologous muscles within the active and non-active limbs for both right and left-handed contractions during MRI scans. Additionally, the primary experiment included two left-handed participants, and there are reports that activation (Begliomini et al., 2008; Grabowska et al., 2012) and connectivity (Pool et al., 2014, 2015) differ between individuals of different hand dominance. To address this potential confound, we reanalyzed these data with the two left-handed participants removed and observed the same effects in each hemisphere, and therefore opted to include the two left-handed participants in the analyses. Future research should consider investigating differences between left and right-handed participants with a similar paradigm. Finally, the lack of cM1 scaling with parametric increases in handgrip force was an unexpected finding that warrants replication in future studies.

This study examined the effects of parametrically increasing handgrip force on brain activation and functional connectivity within the sensorimotor network. While an increase in ipsilateral sensorimotor activation and excitability have been observed in previous literature (Hortobágyi et al., 2003; Kobayashi et al., 2003; Zijdewind et al., 2006; Sun et al., 2007; Perez and Cohen, 2008; Hendy et al., 2017), our data suggest that the cM1 signal change, although greater in magnitude (i.e. % signal change), does not appear to scale with handgrip force to the same extent as the iM1. We present evidence that high force handgrip contractions result in an observable increase in iM1 BOLD signal change that scales with handgrip force. Further, our novel analyses examining the on-task functional connectivity of the sensorimotor network during unimanual handgrip contractions suggest that the sensorimotor network strength as a whole, and within iM1 and cM1 ROI, correlates with relative handgrip force.

CONFLICTS OF INTEREST

None to declare.

DATA AVAILABILITY STATEMENT

The data that support the findings of this study are available upon request from the corresponding author.

FUNDING SOURCES

This study was funded by a Natural Sciences and Engineering Research Council of Canada (NSERC) Discovery Grant: 2016-0529, awarded to Jonathan P. Farthing, in addition to an NSERC Discovery Grant: 183968-2013-22, awarded to Ron Borowsky. Justin W. Andrushko, and Chelsea Ekstrand received NSERC Alexander Graham Bell Canada Graduate Scholarship – Doctoral (CGS D) Awards and Layla Gould received a Saskatchewan Health Research Foundation (SHRF) postdoctoral fellowship to complete this work.

ACKNOWLEDGEMENTS

We would like to thank Dr. Joel Lanovaz, University of Saskatchewan for his guidance with the creation of MATLAB scripts to process the force data and Shawn Reinink, University of Saskatchewan, for his assistance in modifying the LabView software for the experiment.

REFERENCES

Aboodarda SJ, Šambaher N, Behm DG (2016) Unilateral elbow flexion fatigue modulates corticospinal responsiveness in non-fatigued contralateral biceps brachii Available at:. Scand J Med Sci Sport 26:1301–1312. Available from: http://www.ncbi.nlm.nih.gov/pubmed/26633736.

Amaral DG (2000) The functional organization of perception and movement. In: Kandel ER, Schwartz JH, Jessell TM, editors. Principles of Neural Science. New York: McGraw-Hill. p. 337–348.

Andersson JLR, Jenkinson M, Smith S (2007a) Non-linear registration aka spatial normalisation FMRIB Technial Report TR07JA2.

Andersson JLR, Jenkinson M, Smith S (2007b) Non-linear optimisation FMRIB Technial Report TR07JA1.

Beckmann CF, Smith SM (2004) Probabilistic independent component analysis for functional magnetic resonance imaging Available at:. IEEE Trans Med Imaging 23:137–152. Available from: http://www.ncbi.nlm.nih.gov/pubmed/14964560.

Begliomini C, Nelini C, Caria A, Grodd W, Castiello U (2008) Cortical activations in humans grasp-related areas depend on hand used and handedness. PLoS ONE 3.

Bi G, Poo M (2001) Synaptic modification by correlated activity: Hebb's postulate revisited. Annu Rev Neurosci 24:139–166.

Buetefisch CM, Revill KP, Shuster L, Hines B, Parsons M (2014) Motor demand-dependent activation of ipsilateral motor cortex Available at:. J Neurophysiol 112:999–1009. Available from: http://www.ncbi.nlm.nih.gov/pubmed/24848477.

Buschbacher RM, Prahlow ND (2000) Manual of nerve conduction studies. J Clin Neuromuscul Dis 2:120 Available at: http://journals.lww.com/jcnmd/Abstract/2000/12000/Manual_of_Nerve_Conduction_Studies.15.aspx.

Carson RG (2020) Inter-hemispheric inhibition sculpts the output of neural circuits by co-opting the two cerebral hemispheres. J Physiol:JP279793 Available at: https://onlinelibrary.wiley.com/doi/abs/10.1113/JP279793 [Accessed September 22, 2020].

Chen G, Taylor PA, Cox RW (2017) Is the statistic value all we should care about in neuroimaging? Neuroimage 147:952–959.

Cincotta M, Ziemann U (2008) Neurophysiology of unimanual motor control and mirror movements. Clin Neurophysiol 119:744–762.

Cole MW, Ito T, Schultz D, Mill R, Chen R, Cocuzza C (2018) Task activations produce spurious but systematic inflation of task functional connectivity estimates Available at:. Neuroimage 189:1–18. Available from: http://www.ncbi.nlm.nih.gov/pubmed/30597260.

Dai TH, Liu JZ, Saghal V, Brown RW, Yue GH (2001) Relationship between muscle output and functional MRI-measured brain activation. Exp Brain Res 140:290–300.

Dettmers C, Fink GR, Lemon RN, Stephan KM, Passingham RE, Silbersweig D, Holmes A, Ridding MC, Brooks DJ, Frackowiak RSJ (1995) Relation between cerebral activity and force in the motor areas of the human brain. J Neurophysiol 74:802–815.

Doty RW, Negrão N (1973) Forebrain commissures and vision. In: Vision centers in the brain. Berlin, Heidelberg: Springer. p. 543–582.

Eklund A, Knutsson H, Nichols TE (2019) Cluster failure revisited: Impact of first level design and physiological noise on cluster false positive rates. Hum Brain Mapp 40:2017–2032.

Enoka RM, Duchateau J (2008) Muscle fatigue: What, why and how it influences muscle function. J Physiol 586:11–23 Available at: /pmc/articles/PMC2375565/?report=abstract [Accessed September 20, 2020].

Fan L, Li H, Zhuo J, Zhang Y, Wang J, Chen L, Yang Z, Chu C, Xie S, Laird AR, Fox PT, Eickhoff SB, Yu C, Jiang T (2016) The human brainnetome atlas: A new brain atlas based on connectional architecture. Cereb Cortex 26:3508–3526 Available at: http://www.ncbi.nlm.nih.gov/pubmed/27230218 [Accessed April 17, 2020].

Fling BW, Kwak Y, Peltier SJ, Seidler RD (2012) Differential relationships between transcallosal structural and functional connectivity in young and older adults Available at:. Neurobiol Aging 33:2521–2526. Available from: http://www.ncbi.nlm.nih.gov/pubmed/22177217.

Golkowski D, Ranft A, Kiel T, Riedl V, Kohl P, Rohrer G, Pientka J, Berger S, Preibisch C, Zimmer C, Mashour GA, Schneider G, Kochs EF, Ilg R, Jordan D (2017) Coherence of BOLD signal and electrical activity in the human brain during deep sevoflurane anesthesia. Brain Behav 7:e00679 Available at: http://www.ncbi.nlm.nih.gov/pubmed/28729926 [Accessed September 16, 2019].

Grabowska A, Gut M, Binder M, Forsberg L, Rymarczyk K, Urbanik A (2012) Switching handedness: fMRI study of hand motor control in right-handers, left-handers and converted left-handers. Acta Neurobiol Exp (Wars) 72:439–451.

Hebb DO (1949) The first stage of perception: growth of the assembly. Organ Behav 4:60–78.

Hendy AM, Chye L, Teo W-P (2017) Cross-activation of the motor cortex during unilateral contractions of the quadriceps Available at:. Front Hum Neurosci 11.

Hess CW, Mills KR, Murray NMF (1986) Magnetic stimulation of the human brain: Facilitation of motor responses by voluntary contraction of ipsilateral and contralateral muscles with additional observations on an amputee. Neurosci Lett 71:235–240.

Hortobágyi T, Richardson SP, Lomarev M, Shamim E, Meunier S, Russman H, Dang N, Hallett M (2011) Interhemispheric plasticity in humans. Med Sci Sports Exerc 43:1188–1199.

Hortobágyi T, Taylor JL, Petersen NT, Russell G, Gandevia SC (2003) Changes in segmental and motor cortical output with contralateral muscle contractions and altered sensory inputs in humans Available at:. J Neurophysiol 90:2451–2459. Available from: http://www.ncbi.nlm.nih.gov/pubmed/14534271.

Hyvärinen A (1999) Fast and robust fixed-point algorithms for independent component analysis Available at:. IEEE Trans Neural Networks 10:626–634. Available from: http://www.ncbi.nlm.nih.gov/pubmed/18252563.

Jankowska E, Edgley SA (2006) How can corticospinal tract neurons contribute to ipsilateral movements? A question with implications for recovery of motor functions. Neuroscientist 12:67–79.

Jenkinson M, Bannister P, Brady M, Smith S (2002) Improved optimization for the robust and accurate linear registration and motion correction of brain images Available at:. Neuroimage 17:825–841. Available from: http://www.ncbi.nlm.nih.gov/pubmed/12377157.

Jenkinson M, Beckmann CF, Behrens TEJ, Woolrich MW, Smith SM (2012) FSL. Neuroimage 62:782–790 Available at: http://www.ncbi.nlm.nih.gov/pubmed/21979382 [Accessed March 8, 2020].

Jenkinson M, Smith S (2001) A global optimisation method for robust affine registration of brain images Available at:. Med Image Anal 5:143–156. Available from: http://www.ncbi.nlm.nih.gov/pubmed/11516708.

Jiang Z, Wang X-F, Kisiel-Sajewicz K, Yan JH, Yue GH (2012) Strengthened functional connectivity in the brain during muscle fatigue Available at:. Neuroimage 60:728–737. Available from: http://linkinghub.elsevier.com/retrieve/pii/S1053811911014157.

Kim SG, Ashe J, Hendrich K, Ellermann JM, Merkle H, Uğurbil K, Georgopoulos AP (1993) Functional magnetic resonance imaging of motor cortex: Hemispheric asymmetry and handedness. Science (80-) 261:615–617.

Kobayashi M, Hutchinson S, Schlaug G, Pascual-Leone A (2003) Ipsilateral motor cortex activation on functional magnetic resonance imaging during unilateral hand movements is related to interhemispheric interactions Available at:. Neuroimage 20:2259–2270. Available from: http://www.ncbi.nlm.nih.gov/pubmed/14683727.

Lemon R, Kraskov A (2019) Starting and stopping movement by the primate brain. Brain Neurosci Adv 3:239821281983714 Available at: http://journals.sagepub.com/doi/10.1177/2398212819837149 [Accessed June 3, 2020].

Lenth R (2018) emmeans: Estimated marginal means, aka least-squares means. R Package. Available at: https://cran.r-project.org/package=emmeans.

Maier MA, Kirkwood PA, Brochier T, Lemon RN (2013) Responses of single corticospinal neurons to intracortical stimulation of primary motor and premotor cortex in the anesthetized macaque monkey. J Neurophysiol 109:2982–2998.

Maruyama A, Matsunaga K, Tanaka N, Rothwell JC (2006) Muscle fatigue decreases short-interval intracortical inhibition after exhaustive intermittent tasks Available at:. Clin Neurophysiol 117:864–870. Available from: http://linkinghub.elsevier.com/retrieve/pii/S1388245705005250.

Minka TP (2000) Automatic choice of dimensionality for PCA. Technical Report 514. MIT Media Lab Vis Model Gr.

Muellbacher W, Facchini S, Boroojerdi B, Hallett M (2000) Changes in motor cortex excitability during ipsilateral hand muscle activation in humans. Clin Neurophysiol 111:344–349.

Nickerson LD, Smith SM, Öngür D, Beckmann CF (2017) Using dual regression to investigate network shape and amplitude in functional connectivity analyses Available at:. Front Neurosci 11:115. Available from: http://www.ncbi.nlm.nih.gov/pubmed/28348512.

Perez MA, Cohen LG (2008) Mechanisms underlying functional changes in the primary motor cortex ipsilateral to an active hand. J Neurosci 28:5631–5640. Available at: http://www.ncbi.nlm.nih.gov/pubmed/18509024 [Accessed January 28, 2020].

Pool EM, Rehme AK, Eickhoff SB, Fink GR, Grefkes C (2015) Functional resting-state connectivity of the human motor network: Differences between right- and left-handers. Neuroimage 109:298–306.

Pool EM, Rehme AK, Fink GR, Eickhoff SB, Grefkes C (2014) Handedness and effective connectivity of the motor system. Neuroimage 99:451–460.

Pruim RHR, Mennes M, van Rooij D, Llera A, Buitelaar JK, Beckmann CF (2015) ICA-AROMA: A robust ICA-based strategy for removing motion artifacts from fMRI data. Neuroimage 112.

R Core Team (2019) R: A language and environment for statistical computing (Version 3.6). R Found Stat Comput.

Reuter M, Fischl B (2011) Avoiding asymmetry-induced bias in longitudinal image processing. Neuroimage 57:19–21.

Reuter M, Schmansky NJ, Rosas HD, Fischl B (2012) Within-subject template estimation for unbiased longitudinal image analysis. Neuroimage 61:1402–1418.

Rosen A, Stephens J, Glover G, Main K, Boakye M, Fraser P, Lamy JC (2013) Relationship between functional connectivity and interhemispheric inhibition in older adults. Clin Neurophysiol 124:e158–e159.

Salimi-Khorshidi G, Douaud G, Beckmann CF, Glasser MF, Griffanti L, Smith SM (2014) Automatic denoising of functional MRI data: Combining independent component analysis and hierarchical fusion of classifiers. Neuroimage 90:449–468.

Shatz CJ (1992) The developing brain. Sci Am 267:60–67. Available at: http://www.nature.com/doifinder/10.1038/scientificamerican-0992-60 [Accessed March 19, 2020].

Singmann H (2018) afex: Analysis of fractional experiments. R Package. Available at: https://cran.r-project.org/package=afex.

Smith SM (2002) Fast robust automated brain extraction Available at:. Hum Brain Mapp 17:143–155. Available from: http://www.ncbi.nlm.nih.gov/pubmed/12391568.

Smith SM, Fox PT, Miller KL, Glahn DC, Fox PM, Mackay CE, Filippini N, Watkins KE, Toro R, Laird AR, Beckmann CF (2009) Correspondence of the brain's functional architecture during activation and rest. Proc Natl Acad Sci U S A 106:13040–13045.

Smith SM, Nichols TE (2009) Threshold-free cluster enhancement: Addressing problems of smoothing, threshold dependence and localisation in cluster inference. Neuroimage 44:83–98.

Stagg CJ, Bachtiar V, Amadi U, Gudberg CA, Ilie AS, Sampaio-Baptista C, O'Shea J, Woolrich M, Smith SM, Filippini N, Near J, Johansen-Berg H (2014) Local GABA concentration is related to network-level resting functional connectivity Available at:. Elife 3:1–9. Available from: https://elifesciences.org/articles/01465.

Stedman A, Davey NJ, Ellaway PH (1998) Facilitation of human first dorsal interosseous muscle responses to transcranial magnetic stimulation during voluntary contraction of the contralateral homonymous muscle. Muscle Nerve 21:1033–1039. Available at: http://doi.wiley.com/10.1002/%28SICI%291097-4598%28199808%2921%3A8%3C1033%3A%3AID-MUS7%3E3.0.CO%3B2-9 [Accessed June 17, 2020].

Steel A, Song S, Bageac D, Knutson KM, Keisler A, Saad ZS, Gotts SJ, Wassermann EM, Wilkinson L (2016) Shifts in connectivity during procedural learning after motor cortex stimulation: A combined transcranial magnetic stimulation/functional magnetic resonance imaging study Available at:. Cortex 74:134–148. Available from: http://www.ncbi.nlm.nih.gov/pubmed/26673946.

Sun FT, Miller LM, Rao AA, D'Esposito M (2007) Functional connectivity of cortical networks involved in bimanual motor sequence learning. Cereb Cortex 17:1227–1234.

Takahashi K, Maruyama A, Maeda M, Etoh S, Hirakoba K, Kawahira K, Rothwell JC (2009) Unilateral grip fatigue reduces short interval intracortical inhibition in ipsilateral primary motor cortex Available at:. Clin Neurophysiol 120:198–203. Available from: http://linkinghub.elsevier.com/retrieve/pii/S1388245708010092.

The Jamovi Project (2020) Jamovi (Version 1.2). Available at: https://www.jamovi.org.

Thickbroom GW, Phillips BA, Morris I, Byrnes ML, Mastaglia FL (1998) Isometric force-related activity in sensorimotor cortex measured with functional MRI. Exp Brain Res 121:59–64.

Tinazzi M, Zanette G (1998) Modulation of ipsilateral motor cortex in man during unimanual finger movements of different complexities. Neurosci Lett 244:121–124.

Uehara K, Funase K (2014) Contribution of ipsilateral primary motor cortex activity to the execution of voluntary movements in humans: A review of recent studies. J Phys Fit Sport Med 3:297–306.

Van Duinen H, Renken R, Maurits NM, Zijdewind I (2008) Relation between muscle and brain activity during isometric contractions of the first dorsal interosseus muscle. Hum Brain Mapp 29:281–299.

Vercauteren K, Pleysier T, Van Belle L, Swinnen SP, Wenderoth N (2008) Unimanual muscle activation increases interhemispheric inhibition from the active to the resting hemisphere. Neurosci Lett 445:209–213.

Verstynen T, Diedrichsen J, Albert N, Aparicio P, Ivry RB (2005) Ipsilateral motor cortex activity during unimanual hand movements relates to task complexity. J Neurophysiol 93:1209–1222.

Woolrich MW, Ripley BD, Brady M, Smith SM (2001) Temporal autocorrelation in univariate linear modeling of FMRI data Available at:. Neuroimage 14:1370–1386. Available from: http://www.ncbi.nlm.nih.gov/pubmed/11707093.

Worsley K (2001) Statistical analysis of activation images. In: Jezzard P, Matthews PM, Smith SM, editors. Functional MRI: An Introduction to Methods, First edit. Oxford: Oxford University Press. p. 251–270.

Zehr EP (2002) Considerations for use of the Hoffmann reflex in exercise studies. Eur J Appl Physiol 86:455–468.

Zenke F, Gerstner W, Ganguli S (2017) The temporal paradox of Hebbian learning and homeostatic plasticity. Curr Opin Neurobiol 43:166–176.

Zijdewind I, Butler JE, Gandevia SC, Taylor JL (2006) The origin of activity in the biceps brachii muscle during voluntary contractions of the contralateral elbow flexor muscles Available at:. Exp Brain Res 175:526–535. Available from: http://www.ncbi.nlm.nih.gov/pubmed/16924489.

(Received 20 June 2020, Accepted 26 October 2020)
(Available online 13 November 2020)